PISTORIUS, P.G.H., DE KLERK, H.J., and VAN ROOYEN, G.T. The austenite–ferrite transformation in 11,5 per cent chromium steels. *Proceedings of the 6th International Chromium Steel and Alloys Congress, Cape Town.* Volume 2. Johannesburg, SAIMM, 1992. pp. 65–70.

The Austenite–Ferrite Transformation in 11,5 per cent Chromium Steels

P.G.H. PISTORIUS*, H.J. DE KLERK†, and G.T. VAN ROOYEN*

**University of Pretoria, Pretoria, South Africa*
†Iscor Ltd, Pretoria, South Africa

The transformation characteristics of two 11,5 per cent chromium steels with a dual-phase austenite–ferrite microstructure at high temperature were studied to elucidate the influence of titanium stabilization. Although the amount of high-temperature (delta) ferrite varied significantly between the two steels, the difference in the grain-boundary surface area between the austenite and the delta ferrite was fairly small. Isothermal transformation characteristics were evaluated in terms of the Johnson–Mehl–Avrami–Kolmogorov equation $f = 1 - \exp(-k\,(t-t_0)^n)$. The development of the microstructure during isothermal transformation was studied by transmission electron microscopy of samples produced during interrupted isothermal runs.

Two mechanisms for the transformation of austenite to ferrite were observed: the growth of existing delta ferrite into austenite grains, and the nucleation and growth of nascent ferrite. The precipitation of carbides probably preceded the formation of ferrite. The transformation of austenite by the growth of delta ferrite was the dominant mechanism for austenite–ferrite transformation in the titanium-stabilized steel. This could be explained in terms of the higher fraction of delta ferrite present. The influence of the transformation temperature on both the Johnson–Mehl–Avrami–Kolmogorov exponent n and the constant k was considerably more than that resulting from the presence or absence of titanium stabilization. There are indications that n is insensitive to chemical composition. The transformation of austenite to ferrite under continuous-cooling conditions was slightly more sluggish in the titanium-containing steel. The fraction of martensite present after cooling at a specific cooling rate did not differ substantially between the two steels.

Introduction

A corrosion-resistant steel designated 3CR12 is produced by Middelburg Steel & Alloys (Pty) Ltd. This steel[1] contains approximately 11,5 per cent chromium and has a dual-phase austenite–ferrite structure at temperatures between about 800 and 1350°C. Two variants of this steel are produced: a titanium-stabilized steel containing approximately 0,5 per cent nickel (referred to as 3CR12Ti in this work), and a titanium-free steel (3CR12L). Although the total carbon content of the latter product is lower than that of 3CR12Ti, it is largely in interstitial solution owing to the absence of significant amounts of titanium.

The transformation characteristics of austenite are of industrial significance, since they govern the microstructure and mechanical properties of hot-rolled material. The transformation of austenite to ferrite in these two steels was studied by the establishment of the microstructure at various temperatures in the austenite–ferrite field. The isothermal transformation kinetics were determined, and the evolution of the microstructure was studied by means of interrupted isothermal runs. A continuous-cooling transformation (CCT) diagram was established.

Experimental Procedure

The chemical compositions of the two steels are given in Table I.

TABLE I
CHEMICAL COMPOSITION OF MATERIAL STUDIED
(IN PERCENTAGE BY MASS)

Steel	C	Si	Mn	Cr	Ni	N	Ti
3CR12Ti	0,023	0,43	1,25	11,36	0,58	0,020	0,39
3CR12L	0,010	0,38	1,04	11,28	0,11	0,019	0,002

Heat treatment for this study was done in a tube-furnace dilatometer of low thermal mass. A cylindrical specimen with a diameter of approximately 3 mm and a length between 15 and 25 mm was used. During the construction of the tube furnace, the temperature difference along the length of the specimen was checked by means of a differential thermocouple. Under steady or slow cooling or heating conditions, the temperature difference along the full length of the specimen was always below 10°C and usually below 5°C. During a heat-treatment cycle, the specimen temperature was continuously recorded by use of a spot-

welded intrinsic noble-metal thermocouple of 0,1 mm diameter. The length change was recorded by use of a silica push rod coupled to a linear variable differential transformer (LVDT) core. The specimen and the push rod were contained in a hermetically sealed silica-glass tube. The resistively heated furnace was controlled by use of a second thermocouple and a programmable furnace controller. The fastest cooling rate that could be achieved with this apparatus was about 2 $K \cdot s^{-1}$. This was adequate to characterize the austenite–ferrite transformation due to the high hardenability of this material.

The high-temperature microstructure was established for a wide range of temperatures and times at maximum temperature. This was done to establish the sensitivity of the results to variations in the heat-treatment procedure. After cooling at a rate rapid enough to ensure that all the austenite was transformed to martensite, the specimens were prepared for metallographic examination. A system of image analysis coupled to a scanning electron microscope was used to quantify the very fine microstructure[2].

For both the isothermal and the continuous-cooling heat treatments, an initial temperature of 1000°C was maintained for 10 minutes. This temperature corresponded to the reheating temperature before the final rolling pass. Subsequently, the furnace was allowed to cool rapidly to either the isothermal transformation temperature or, in the case of the continuous-cooling runs, to 820°C followed by cooling at a controlled rate. The latter temperature corresponded to the temperature at which rolling was completed.

During the isothermal runs, the length change was measured continuously. This was then interpreted in terms of the Johnson–Mehl–Avrami–Kolmogorov (JMAK) equation[3]:

$$f = 1 - \exp(-k\,(t-t_o)^n), \qquad [1]$$

with f = the fraction of austenite transformed
k = pre-exponential constant
n = JMAK exponent
t_o = incubation time.

This equation was derived under the assumption of constant rates of nucleation and growth. These assumptions are often not valid, reducing the constants to empirical values[4] that describe the kinetics of the transformation.

Results and Discussion

It is clear from the results of the study of the high-temperature austenite–ferrite equilibrium that the 3CR12Ti contained significantly less austenite than the 3CR12L at any given temperature (Figure 1). This may be due to the fact that titanium promotes the formation of carbonitrides, removing carbon and nitrogen (both powerful austenite-stabilizing elements) from interstitial solution. In both steels, the austenite fraction is fairly insensitive to both temperature and time at temperatures over a range of about 60°C, ranging from about 970 to 1030°C and a variation in the duration of heat treatment ranging from 10 minutes up to at least 1 hour. Equilibrium is probably reached fairly quickly at these high temperatures, as previously pointed out[1]. This implies that the actual temperature of the austenitization heat treatment did not have to be controlled within a particularly narrow band to give reproducible results, in terms of the relative amounts of austenite and ferrite at least.

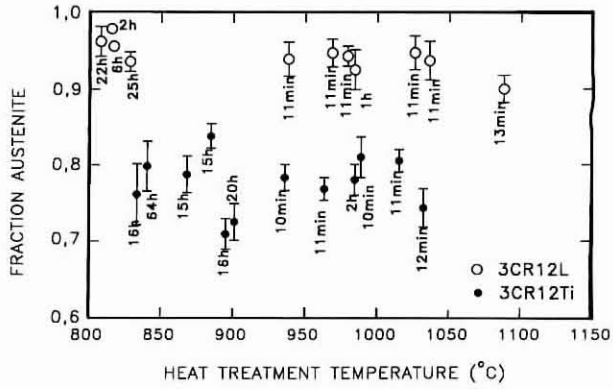

FIGURE 1. Influence of temperature and time on the balance between the austenite and delta-ferrite phases

The high-temperature microstructure was also characterized in terms of the grain-boundary surface between the austenite (martensite after quenching) and the ferrite (Figure 2). Although the reliability of the estimates for this feature seemed considerably lower than that for the volume fraction of austenite at the austentization temperature, it should be noted that the full range extending from 20 to 180 mm^2/mm^3 corresponds to approximately two ASTM grain-size numbers. Although some coarsening of the high-temperature microstructure (with the concomitant decrease in the surface area of the austenite–ferrite grain boundary) did occur when the austenitization temperature was maintained for more than 1 hour, this microstructural feature was, like the austenite volume fraction, not unduly sensitive to the actual heat treatment. The difference between the titanium-stabilized and the titanium-free material in terms of the austenite–ferrite grain-boundary surface area was not as obvious as the difference in the volume fraction of the austenite present.

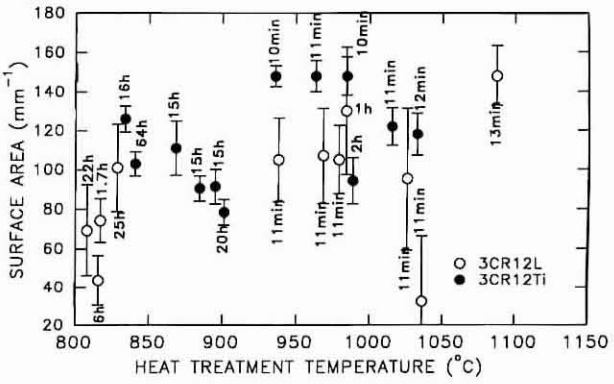

FIGURE 2. Influence of temperature and time on the grain-boundary surface area of the austenite–delta ferrite

The transformation of austenite to ferrite can occur by several mechanisms, two of which are the nucleation and growth of nascent ferrite on sites such as austenite grain corners and edges, and the growth of high-temperature (delta) ferrite into the austenite. If the latter mechanism plays a dominant role, steels with a similar austenite–ferrite grain-boundary surface area would exhibit similar transformation characteristics.

The isothermal transformation behaviour as determined for these two steels qualitatively confirmed previous results on high-purity Fe–10%Cr alloys[5] and 13 per cent chromium steels[6], in that the transformation was sluggish but the incubation time was short, often only a few minutes. The austenite–ferrite transformation in dual-phase 16 to 18 per cent chromium steels was described as starting after a short incubation time of 10 to 20 seconds, after which precipitation at austenite–ferrite grain boundaries started. Ferrite formed from the austenite only after precipitation. This means that precipitates would demarcate grain boundaries between austenite and delta ferrite where initial $\gamma \rightarrow \alpha$ transformation had taken place.

The isothermal runs were evaluated in terms of the JMAK equation. The necessary parameters were estimated by means of a constrained nonlinear optimization procedure. That this equation yielded an adequate description of an actual isothermal transformation was obvious from the linear plot of ln (–ln (1–f)) vs ln (t–t_o), also known as the JMAK plot (Figure 3). For most transformation temperatures, the JMAK plot was fairly linear, but some deviation from linearity was apparent at transformation temperatures above about 670°C.

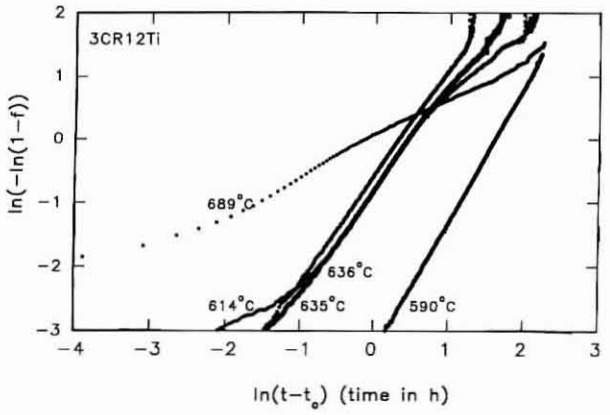

FIGURE 3. JMAK plot for the isothermal transformation of austenite to ferrite

The two JMAK plots for transformation at 635°C represent the behaviour of hot-rolled ferrite–martensite and fully ferritic ferrite–carbide starting microstructures before being heated to the austenitizing temperature. Apart from a small discrepancy during the initial stages of transformation (with ln (–ln (1–f)) < –2,5 , or f < 0,08), the transformation behaviour of this material seems to be largely insensitive to the starting microstructure. This indicated that repeated heat treatments of the same specimen, which occurred fairly often while the transformation behaviour was being established under continuous-cooling conditions, probably did not have a major effect.

Another way to check the validity of the JMAK equation would be to compare the rate of austenite–ferrite transformation as predicted by this equation with the experimentally determined transformation rate. The former is given by

$$f' = k\, n(t\text{-}t_o)^{(n-1)} \exp(-k\,(t\text{-}t_o)^{n}). \qquad [2]$$

As shown in Figure 4, the discrepancy between these two functions describing the transformation rate could be largely due to experimental noise, which was exacerbated by differentiating experimental data.

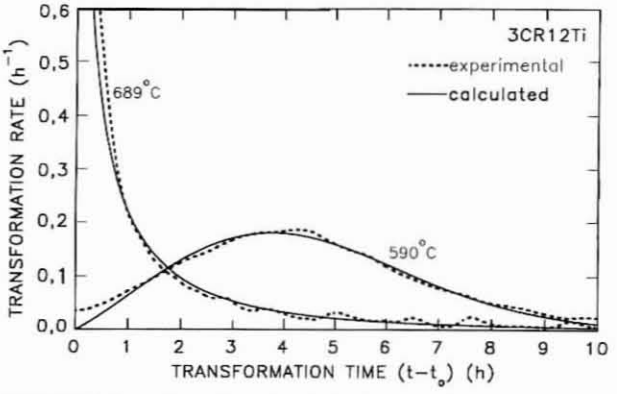

FIGURE 4. Rate of transformation during isothermal transformation of austenite to ferrite

Interruption of the isothermal transformation of austenite to ferrite at around 600°C early in the transformation period by rapid cooling to room temperature after about 3 hours resulted in the typical microstructure shown in Figure 5. Two grains of delta ferrite and a grain of austenite (now martensite) were bordered by a grain boundary now demarcated by a band of fine precipitates. Such precipitates are expected to coarsen during long isothermal periods, and further precipitation can be expected. These features are shown in Figure 6. The pinning of the austenite–ferrite grain boundary by precipitates inside the austenite seems to result in a highly serrated grain boundary. Dark-field microscopy showed the fibrous phase in the ferrite to consist of some residual austenite, but mainly of precipitates similar to the coarser species further away from the austenite–ferrite grain boundary.

The transformation of austenite by the migration of the grain boundaries between the austenite and the delta ferrite was clearly of significance in the transformation of austenite to ferrite.

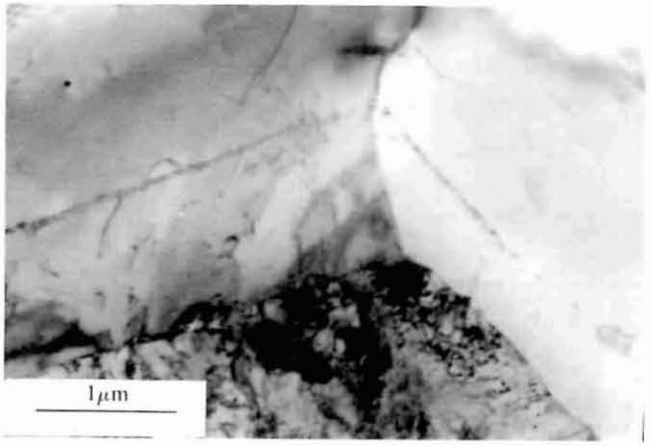

FIGURE 5. Movement of the austenite–ferrite grain boundary in 3CR12Ti during initial stages of isothermal transformation at 600°C

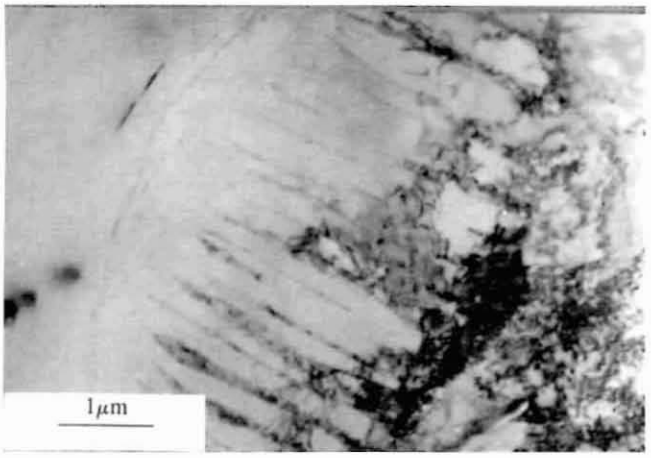

FIGURE 6. The austenite–ferrite grain boundary in 3CR12Ti during later stages of isothermal transformation at 600°C

When full isothermal transformation of the austenite was allowed, there was significant carbide coarsening (Figure 7). These precipitates occurred in strings, probably associated with the high-temperature austenite–delta ferrite grain boundaries. The formation of coarse precipitates at higher isothermal transformation temperatures may play a role in the nonlinear JMAK behaviour exhibited at these temperatures.

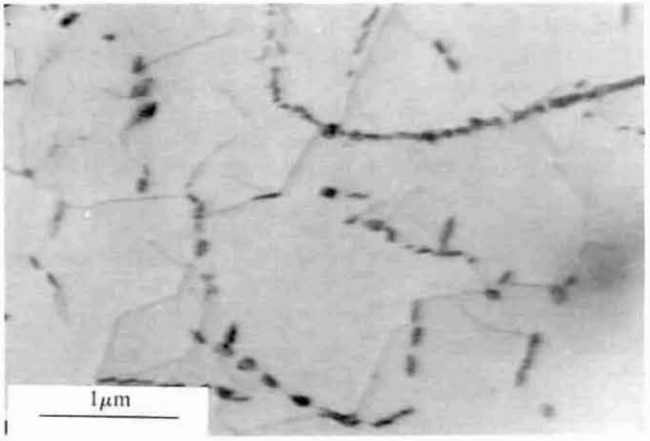

FIGURE 7. Heavy precipitation after isothermal transformation of 3CR12Ti at 700°C

The 3CR12L material studied contained significantly less ferrite at approximately 1000°C than did the 3CR12Ti material. The transformation of austenite to ferrite by a nucleation and growth mechanism would therefore be expected to be more dominant in 3CR12L material. The nucleation of ferrite at the edge of an austenite grain in titanium-free material after an isothermal period of 4 hours at 600°C (as shown in Figure 8) was not observed in the titanium-stabilized material. Serrations of the austenite–ferrite grain boundary were observed, although not in all the grain boundaries of this type. It is clear that the serrations were associated with the lath structure in the martensite, which formed from the austenite at the end of the isothermal period. These laths were probably nucleated at the austenite–ferrite grain boundary, and may not be an indication of a substructure in the austenite in front of the advancing ferrite grain boundary. A possible explanation for these serrations would be the presence of precipitates in the austenite itself. These precipitates would have to be very fine to cause the severe pinning shown particularly in Figure 6 but also in Figure 8. Similar structures were demonstrated, by high-temperature high-voltage electron microscopy, of the growth of ferrite in Fe–0,35%C–0,9%Mo steels. The Mo_2C precipitates formed as rows or as fibres on the advancing austenite–ferrite boundaries[7].

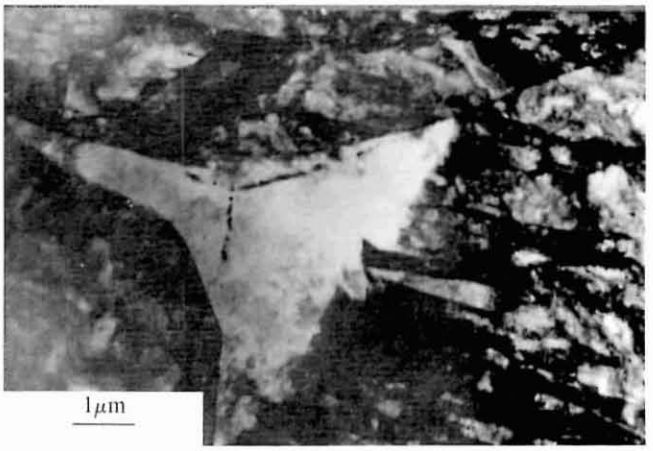

FIGURE 8. Possible ferrite nucleus at an austenite grain-boundary triple point

The kinetics of the isothermal transformation as described in terms of the JMAK exponent n are shown in Figure 9. Also shown are data for the transformation of a 0,34 per cent carbon steel from a fully austenitic structure to ferrite and pearlite[8]. The similarity between the results for the two 11,5 per cent chromium steels studied are obvious, and somewhat surprising given the difference in volume fraction of delta ferrite present at high temperatures, and the fact that the grain boundaries between austenite and delta ferrite seemed fairly inactive during the transformation of austenite in the titanium-free material. The close agreement between the values of the JMAK exponent for the transformation of austenite in 11,5 per cent chromium steels and for the transformation of an Fe–0,34%C austenite to pearlite is somewhat surprising, given the difference in chemical composition and high-temperature phases, but could be taken as further evidence of the dominant role of carbide precipitation in the transformation of austenite in 3CR12 steels. It is also clear that the JMAK exponent is fairly insensitive to chemical composition.

The dependence of the pre-exponential constant in the JMAK equation on the temperature is often shown as an Arrhenius plot. From Figure 10 it is clear that the Arrhenius plot is curved. This is usually interpreted as a change in activation energy with transformation temperature[9]. This would mean a change from an activation energy for the transformation of austenite to ferrite and carbides from around 60 $kJ \cdot mol^{-1}$ at high temperatures to around 300 $kJ \cdot mol^{-1}$ at lower transformation temperatures. A more

fundamental approach questions the validity of the quantification of kinetic behaviour by use of the Arrhenius equation in this way[10].

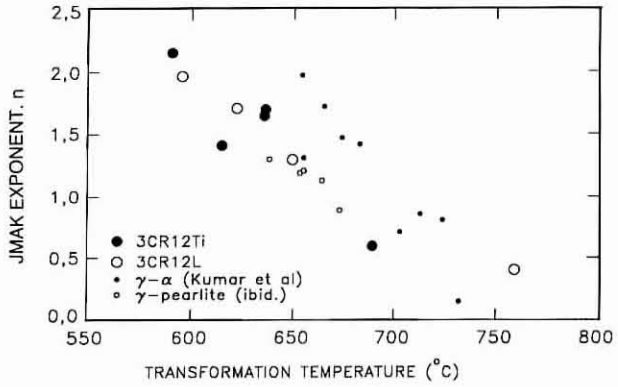

FIGURE 9. JMAK exponent n for the transformation of austenite

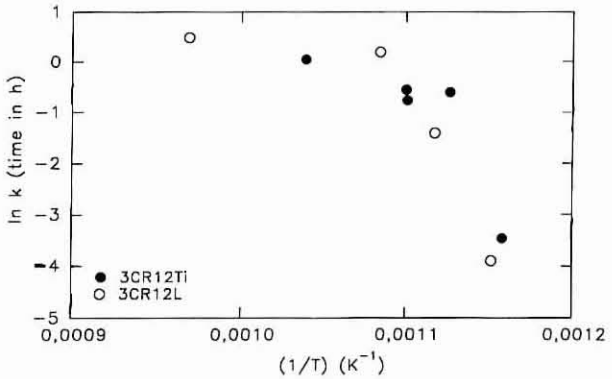

FIGURE 10. Pre-exponential constant k as a function of reciprocal absolute transformation temperature

While the kinetics of isothermal transformations are useful for providing insight into the behaviour of these steels, the continuous-cooling transformation behaviour is of much more immediate industrial significance. The continuous-cooling transformation (CT) diagrams for both steels are given in Figure 11. The hardenability of the titanium-stabilized material was higher than that of the titanium-free material. This could be explained in terms of the lower carbon, nickel, and manganese contents of the latter material. The M_s and M_f temperatures of the titanium-stabilized material were considerably higher than those of the titanium-free material. While 3CR12 exhibited a slight decrease in the M_s and M_f temperatures with an increased fraction of ferrite formed, the titanium-stabilized material showed a dramatic rise in these two temperatures once the cooling rate was slow enough for ferrite to form. The reason for this behaviour is not clear.

The microstructure formed during continuous cooling at various transformation rates for the two steels is shown in Figure 12. The higher hardenability of the titanium-stabilized material caused the curve describing the change in ferrite fraction with cooling rate to shift to slightly lower cooling rates. This material contained more delta ferrite at high temperatures. The difference in the total amount of ferrite after cooling at a specific rate was therefore influenced only slightly by the presence of titanium in the steel, with the largest difference in the fraction of ferrite present at any given cooling rate being around 0,2.

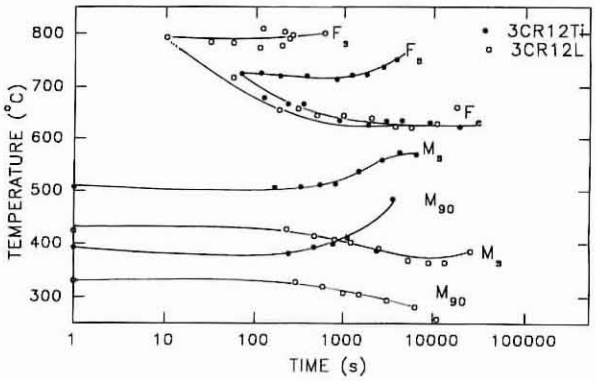

FIGURE 11. Continuous-cooling transformation diagram for 3CR12Ti and 3CR12L

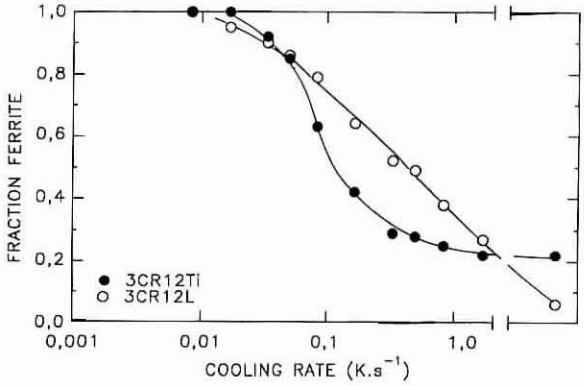

FIGURE 12. The martensite–ferrite phase balance achieved after continuous-cooling transformation at various rates

Conclusions

(1) The high-temperature microstructure in the vicinity of 1000°C is fairly insensitive to temperature. The 3CR12Ti material had a significantly higher fraction of high-temperature (delta) ferrite. The grain-boundary surface area between the austenite and ferrite was not significantly different for the two steels studied.

(2) The isothermal transformation kinetics could be described in terms of the JMAK equation ($f = 1\text{-}\exp(\text{-}k\ (t\text{-}t_o)^n)$). The JMAK plot was linear at transformation temperatures below 670°C. At higher temperatures, significant deviations from linear behaviour were observed. The JMAK equation appropriately predicted the rate of the transformation of austenite to ferrite.

(3) The pre-exponential exponent k and the JMAK exponent n were much more sensitive to the transformation temperature than to the presence of titanium in the steel. There are indications that n is insensitive to chemical composition.

(4) Austenite seemed to be transformed either by the growth of delta ferrite into austenite grains or by the nucleation and growth of nascent ferrite. The latter mechanism seemed to be favoured by the titanium-free material, which contained less delta ferrite.

(5) Precipitates formed during the initial stages of transformation. Coarsening of precipitates, interface precipitation, and heavy pinning of ferrite grain boundaries during the later stages of transformation were observed.

(6) The ferrite 'nose' on the continuous-cooling transformation diagram shifted to somewhat longer times for the titanium-stabilized steel. This could be due to the significant nickel content of that steel. The amount of ferrite formed during continuous-cooling transformation at a specific cooling rate was again not very sensitive to titanium stabilization.

Acknowledgments

The support of the Director of Research of the University of Pretoria, Middelburg Steel & Alloys, and the Research and Development Division of Iscor Ltd is gratefully acknowledged.

References

1. Ball, A., *et al.* (1987). Microstructure, phase equilibria and transformations in corrosion resistant dual phase steel designated 3CR12. *Mater. Sci. Technol.*, 3, pp. 189-196.
2. Pistorius, P.G.H., and Botha, A.J. (1991). Quantitative metallography of the dual phase structure of a 12%Cr steel using scanning electron microscopy. Proceedings of the 30th Conference of the Electron Microscopy Society of Southern Africa.
3. Price, C.W. (1990). Use of Kolmogorov–Johnson–Mehl–Avrami kinetics in the recrystallisation of metals and crystallisation of metallic glasses. *Acta Metall. Mater.*, 5, pp. 727-738.
4. Hutchinson, B., *et al.* (1989). On the kinetics of recrystallisation in cold worked metals. *Scripta Metall.*, 23, pp. 671-676.
5. Bee, J.V., *et al.* (1978). The isothermal decomposition of austenite in a high purity iron–chromium binary alloy. *Metall. Trans.* A, 9A, pp. 587-593.
6. Koepke, W., *et al.* (1970). Untersuchung zum Umwandlungsverhalten 13%iger Chromstäle mit geringen Kohlenstoffgehalt. *Neue Hütte*, 15, pp. 165-170.
7. Purdy, G.R. (1978). The dynamics of transformation interfaces in steels. II. Transformations in Fe–C–Mo alloys at intermediate temperatures. *Acta Metall.*, 26, pp. 487-498.
8. Kumar, A., *et al.* (1991). Modelling thermal and microstructural evolution on runout table of hot strip mill. *Mater. Sci. Technol.*, 7, pp. 360-368.
9. Smith, J.J., Perry, C., and Farrar, R.A. (1990). Development of a new 304L austenitic welding consumable containing tungsten. *J. Mater. Sci.*, 25, pp. 1275-1284.
10. Garn, P.D. (1978). Kinetic parameters. J. *Thermal Anal.*, 13, pp. 581-593.